Electronic transport through a double quantum dot in the spin blockade regime: Theoretical models

Jesús Iñarrea[1,2], Gloria Platero[2] and Allan H. MacDonald[3]
[1] *Escuela Politécnica Superior,Universidad Carlos III,Leganes,Madrid,Spain*
[2] *Instituto de Ciencia de Materiales, CSIC, Cantoblanco,Madrid,28049,Spain.*
[3] *Department of Physics, University of Texas at Austin.Austin, Texas 78712*
(Dated: February 6, 2008)

We analyzed the electronic transport through a double quantum dot in the spin blockade regime. Experiments of current rectification by Pauli exclusion principle in double quantum dots were discussed. The electron and nuclei spin dynamics and their interplay due to the Hyperfine interaction were self-consistently analyzed within the framework of rate equations. Our results show that the current leakage experimentally observed in the spin-blockade region, is due to spin-flip processes induced by Hyperfine interaction through Overhauser effect. We show as well how a magnetic field applied parallel to the current allows excited states to participate in the electronic current and removes spin blockade. Our model includes also a self-consistent description of inelastic transitions where the energy is exchanged through interactions with acoustic phonons in the environment. It accounts for spontaneous emission of phonons which results in additional features in the current characteristics. We develop a microscopical model to treat the Hyperfine interaction in each dot. Using this model we study the dynamical nuclear polarization as a function of the applied voltage.

PACS numbers:

I. INTRODUCTION

Recent transport experiments in vertical double quantum dots (DQD's) show that Pauli exclusion principle is important[1] in current rectification. In particular, spin blockade (SB) is observed at certain regions of dc voltages. The interplay between Coulomb and SB can be used to block the current in one direction of bias while allowing it to flow in the opposite one. Johnson et al.[2] observed as well SB and spin rectification in a lateral DQD. Then DQD's could behave as externally controllable spin-Coulomb rectifiers with potential application in spintronics as spin memories and transistors.

Spin de-coherence[3, 4] and relaxation processes induced, for instance, by spin-orbit (SO) scattering [5] or Hyperfine (HF) interaction [6], have shown to reduce SB producing a leakage current. In this paper we theoretically analyze recent experiments of transport through two weakly coupled QD's [1]. We consider simultaneously Hyperfine (HF) interaction and emission of phonons to be responsible of the SB lifting and the main features in the experimental current/voltage (I/V_{DC}) curve. According to our calculations, inter-dot phonon-assisted tunneling has to be included to have a full understanding of the physics behind the experimental results. In the corresponding experiment[1], the total electron number of the system is fluctuating between one and two. Due to the different gates voltages applied between the two dots the left dot (n_1) can have up to one electron and the right one (n_2) can fluctuate between one and two keeping the sum ($n_1 + n_2$) between one and two. Current flow is allowed when the electrons in each QD have antiparallel spins and a finite gate voltage allows one electron in the left dot to tunnel sequentially to the right one and further to the collector. However, for weakly coupled QD's there is a similar probability for the electron coming from the left lead to be parallel or antiparallel to the electron spin occupying the right dot. In the first case, the electron cannot tunnel to the right dot due to Pauli exclusion principle and SB takes place, presenting a plateau in the I/V_{DC} curve.

The theoretical model presented in this paper has been developed in the frame of rate equations. We solve self-consistently a system of coupled time-evolution equations for electronic charge occupations and nuclei polarizations. Our theoretical results reproduce the I/V_{DC} observed plateau due to SB and also the main current peaks. HF interaction is proposed as the candidate to lift SB, producing spin-flip (sf) of electrons and nuclei. On the other hand phonon-assisted tunneling is proposed, in parallel with the direct tunneling, to sustain the total current through the device. The electrons and nuclei spin interactions brings to the Overhauser effect, which is also called flip-flop interaction because each time the electron flip the spin up to down (down to up) the nuclear spin does the opposite. According to measurements on QD's by Fujisawa et al.[3] the spin-flip time, $\tau_{sf} > 10^{-6}$s, is much longer than the typical tunneling time, $\tau_{tun} = 1 - 100$ ns, or the momentum relaxation time, $\tau_{mo} = 1 - 10$ ns, meaning that spin-flip processes due to HF interaction are important mostly in the SB region. Our system consists of a vertical DQD under an external DC voltage in the presence of a magnetic field parallel to the current.

II. THEORETICAL MODEL

Elastic and inelastic tunneling

We consider a hamiltonian: $H = H_L + H_R + H_T^{LR} + H_{leads} + H_T^{l,D}$ where $H_L(H_R)$ is the hamiltonian for the isolated left (right) QD and is modelled as one-level (two-level) Anderson impurity. $H_T^{LR}(H_T^{l,D})$ describes tunneling between QD's (leads and QD's)[7]) and H_{leads} is the leads hamiltonian. We use a basis that contains 20 states given by:

$$|1\rangle = |0,\uparrow\rangle; |2\rangle = |0,\downarrow\rangle; |3\rangle = |\uparrow,\uparrow\rangle; |4\rangle = |\downarrow,\downarrow\rangle;$$
$$|5\rangle = |\uparrow,\downarrow\rangle; |6\rangle = |\downarrow,\uparrow\rangle; |7\rangle = |0,\uparrow\uparrow^*\rangle; |8\rangle = |0,\downarrow\downarrow^*\rangle;$$
$$|9\rangle = |0,\uparrow\downarrow\rangle; |10\rangle = |\uparrow,0\rangle; |11\rangle = |\downarrow,0\rangle; |12\rangle = |0,\uparrow^*\rangle;$$
$$|13\rangle = |0,\downarrow^*\rangle; |14\rangle = |\uparrow,\uparrow^*\rangle; |15\rangle = |\downarrow,\downarrow^*\rangle;$$
$$|16\rangle = |\uparrow,\downarrow^*\rangle; |17\rangle = |\downarrow,\uparrow^*\rangle; |18\rangle = |0,0\rangle;$$
$$|19\rangle = |0,\downarrow,\uparrow^*\rangle; |20\rangle = |0,\uparrow\downarrow^*\rangle$$

We have considered two levels in the right QD. Those states marked with (*) correspond to the excited state in the right QD. Double occupied states in the left QD do not participate in the electron transport except for high reverse bias. For simplicity we do not consider here this regime. The system of equations of motion for state occupation probabilities ρ_s includes scattering in and scattering out contributions[7, 8, 9, 10]:

$$\dot{\rho}(t)_s = \sum_{m\neq s} W_{sm}\rho_m - \sum_{k\neq s} W_{ks}\rho_s \qquad (1)$$

Our neglect of coherence[7] effects is appropriate for weakly coupled quantum dots. $W_{i,j}$ is the transition rate state j to state i.

For the contact-QD tunneling rate $W_{i,j}$ we use a Fermi Golden Rule (FGR) expression, i.e., first order time-dependent perturbation theory [11, 12, 13]. The expression for the left contact-QD tunneling reads:

$$W_{L,1(1,L)} = \frac{\pi}{\hbar}T^2\rho\left[\frac{1}{2} + (-)\frac{1}{\pi}arctg\left(\frac{\mu_L - \mu_1 + eV_{L1}}{\gamma}\right)\right] \qquad (2)$$

where $W_{L,1(1,L)}$ is the tunneling probability for the left contact (QD) to the left QD (contact) . A similar expression can be obtained for the the right QD to the right contact:

$$W_{R,2(2,R)} = \frac{\pi}{\hbar}T^2\rho\left[\frac{1}{2} + (-)\frac{1}{\pi}arctg\left(\frac{-\mu_R + \mu_2 - eV_{2R}}{\gamma}\right)\right] \qquad (3)$$

T is the transmission amplitude of the outer barriers, ($T \simeq 1.3\times10^{-3}meV$). γ is the width of the QD state. $\mu_{L,(R)}$ is the chemical potential in the left contact (right) ($\mu_L = 4meV$, $\mu_R = 4meV$ for zero bias[1]), $\mu_{1,(2)}$ is the chemical potential in the left dot (right dot). To calculate $\mu_{1,(2)}$ we have used, apart from the corresponding voltage drops through the device, the intradot and interdot charging energies: 4 and 2 meV respectively[1]. ρ the two-dimensional density of states, V_{L1} is the potential drop between the emitter (left contact) and the left QD and V_{2R} is the potential drop between the right dot and the collector (right contact).

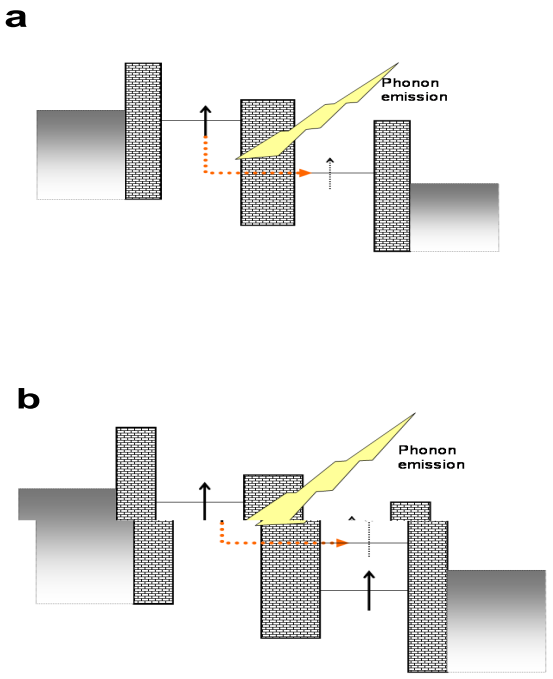

FIG. 1: (Color on line). Schematic diagrams for inelastic phonon-assisted tunneling between weakly coupled dots. a) Between ground levels in each QD. b) Between the ground level of the left QD and the first excited level of the right QD.

Inter-dot transition rates account for both elastic tunneling and inelastic phonon assisted tunneling. The corresponding expression for the elastic inter-dot tunneling is given by:

$$W_{1,2(2,1)} = \frac{T_{1,2}^2}{\hbar}\left[\frac{\gamma}{(\mu_1 - \mu_2 + eV_{12})^2 + \gamma^2}\right] \qquad (4)$$

where $T_{1,2}$ is the transmission through the inner barrier ($T_{1,2} \simeq 5\times10^{-2}meV$) and V_{12} is the voltage drop between the QD's.

For inelastic transitions, energy is exchanged with phonons in the environment. In other words, at $T \approx 0$ (we have considered zero temperature in our calculations) the inelastic tunneling between the two dots is assisted by the emission of acoustic phonons, yielding a significant contribution to the current. This contribution has been experimentally measured by Fujisawa et al.,[14] and

theoretically analyzed by Brandes et al.,[18]. In order to calculate the inelastic transition rate $W_{1,2}^{ph}$ due to the emission of phonons, we have considered the theory developed by Brandes et al.,[18]. Including piezoelectric and deformation potential acoustic phonons the transition rate reads:

$$W_{1,2}^{ph} = \frac{\pi T_{12}^2}{\hbar}\left[\frac{\alpha_{pie}}{\varepsilon} + \frac{\varepsilon}{\hbar^2 w_\xi^2}\right]\left[1 - \frac{w_d}{w}\sin\frac{w}{w_d}\right] \quad (5)$$

where α_{pie} is a piezoelectric coupling parameter ($\alpha_{pie} = 0.02$), $\varepsilon = \hbar w = \mu_1 - \mu_2 + eV_{12}$, $w_d = c/d$ being c the sound velocity and d the distance between the dots. Finally,

$$\frac{1}{w_\xi^2} = \frac{1}{\pi^2 c^3}\frac{\Xi^2}{2\rho_M c^2 \hbar} \quad (6)$$

where ρ_M is the mass density and Ξ is the deformation potential ($\Xi \simeq 7eV$ for GaAs). In Fig. 1, we represent schematically the inelastic contribution to I through the emission of phonons, between the corresponding levels of each QD.

Microscopical model for Hyperfine interaction

We calculate the electronic spin-flip scattering rate $W_{i,j}^{sf}$ using a microscopic model that accounts for HF interactions and external magnetic fields:

$$\hat{H} = g_e\mu_B\vec{S}\cdot\vec{B} + \frac{A}{N_{L(R)}}\sum_{i=1}^{N_{L(R)}}\left[S_z I_z^i + \frac{1}{2}(S_+ I_-^i + S_- I_+^i)\right] \quad (7)$$

where A is the average HF coupling constant, ($A = 90\mu eV$ for GaAs [19]) and I the nuclear spin . $N_{L(R)}$ is the number of nuclei in the left (right) dot, ($N_L = 10^6$ and $N_R = 1.1 \times 10^6$). For simplicity we assume that $I = 1/2$. We take B to be oriented along the $\hat{z}$ direction (current direction). The HF interaction can then be separated into mean-field and flip-flop contributions:

$$\hat{H} = \hat{H}_z + \hat{H}_{sf} \quad (8)$$

where

$$\hat{H}_z = [g_e\mu_B B + A\langle I_z\rangle_{L(R)}]S_z \quad (9)$$

being,

$$\begin{aligned}\langle I_z\rangle_{L(R)} &= \frac{1}{N_{L(R)}}\sum_{i=1}^{N_{L(R)}}(I_z^i)_{L(R)} \\ &= \left[\frac{N^\uparrow - N^\downarrow}{N^\uparrow + N^\downarrow}\right]_{L(R)}|I_z| \\ &= P_{L(R)}|I_z| \end{aligned} \quad (10)$$

$P_{L(R)} = \left[\frac{N^\uparrow - N^\downarrow}{N^\uparrow + N^\downarrow}\right]_{L(R)}$ is the nuclear spin polarization where $N^{\uparrow(\downarrow)}$ is the number of nuclei with spin up(down), in a QD. We have chosen that initially, the nuclei polarization of the left and right dots are equal to zero.

$\hat{H}_z$ has external and effective nuclear field contributions. The latter given by:

$$B_{nuc} = \frac{A\langle I_z\rangle_{L(R)}}{g_e\mu_B} \quad (11)$$

On the other hand:

$$\hat{H}_{sf} = \frac{A}{2N_{L(R)}}\sum_i\left[S_+ I_-^i + S_- I_+^i\right] \quad (12)$$

is the flip-flop interaction responsible for mutual electronic and nuclear spin flips. Nuclei in similar quantum dots can give rise to different effective nuclear fields. This can be related with different effective Hyperfine interactions in each dot. An slightly distinct number of nuclei can explain the different Hyperfine interactions and eventually the independent behavior in terms of the effective nuclear fields. Our model accounts for this situation with $N_{L(R)}$ and $\langle I_z\rangle_{L(R)}$.

Because of the mismatch between nuclear and electronic Zeeman energies spin-flip transitions must be accompanied at low temperature by phonon emission[20]. Phonon absorption is not possible at low temperature. Therefore for $B \neq 0$ Hyperfine interaction only produces electronic spin-flip *relaxation* processes. We approximate the current-limiting spin-flip transition rate from parallel-spin to opposite-spin configurations by:

$$\left[\frac{1}{\tau_{sf}}\right]_{L(R)} \simeq \frac{2\pi}{\hbar}|<\hat{H}_{sf}>|^2\frac{\gamma}{(\Delta Z_e)_{L(R)}^2 + \gamma^2} \quad (13)$$

where the width γ is the electronic state life-time broadening which is of the order of μeV ($\gamma \simeq 5\mu eV$), i.e., of the order of the phonon scattering rate [3]. This equation shows that a different number of nuclei or different splitting Zeeman can give rise to a different spin-flip rate in each dot.

The splitting Zeeman is given by:

$$(\Delta Z_e)_{L(R)} = g_e\mu_B B + \frac{A}{2}P_{L(R)} \quad (14)$$

is the total electronic Zeeman splitting including the Overhauser shift produced by the effective nuclear B.

$$(\Delta Z_{Overhauser})_{L(R)} = \frac{A}{2}P_{L(R)} \quad (15)$$

We assume that a weakly coupled QD's model do no consider molecular states. The basis of states considered reflects this situation. As a consequence, the exchange coupling constant is zero and the Zeeman splitting is given by equation (14).

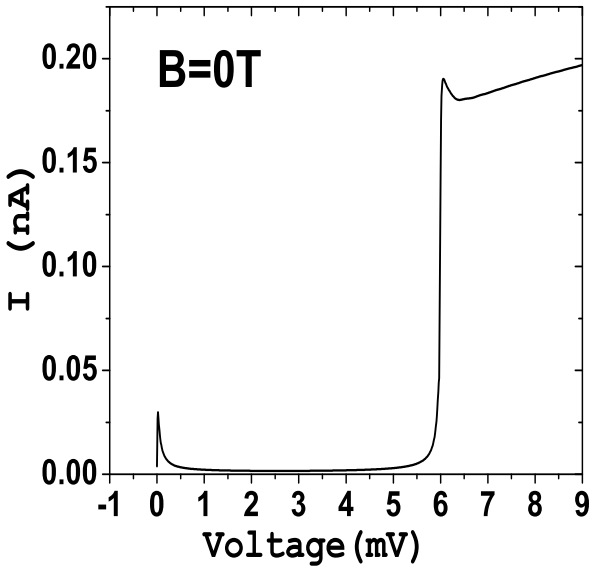

FIG. 2: Stationary I/V_{DC} (B=0). At low V_{DC}, I takes place when one electron from the (1,1) spin-singlet, tunnels to the double occupied singlet state in the right QD (0,2). At higher V_{DC} the system reaches the states $|3\rangle = |\uparrow,\uparrow\rangle$ and $|4\rangle = |\downarrow,\downarrow\rangle$ (inter-dot triplet states) and I drops off due to SB. The SB region is the plateau between the two main peaks, where a finite current leakage is observed due to spin-flip induced by Hyperfine interaction. At larger V_{DC} ($V_{DC} \geq 6$ meV) the chemical potential of the right lead crosses the inter-dot triplet state and the right QD becomes suddenly discharged producing a large peak in I.

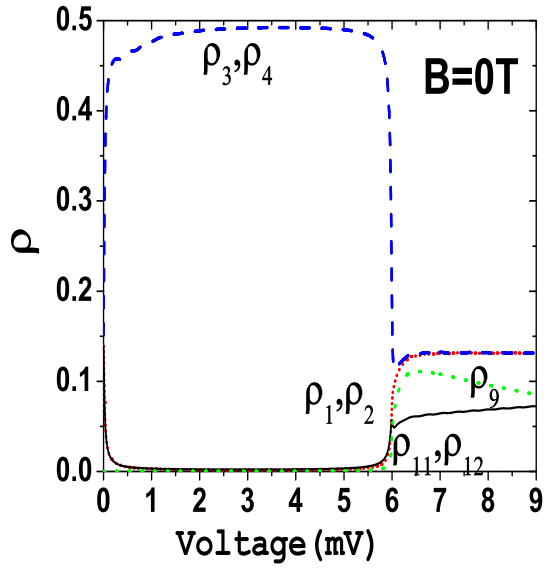

FIG. 3: (Color on line). States occupations versus V_{DC} for $B = 0$. In the SB region the occupation probabilities are dominated by states $|3\rangle = |\uparrow,\uparrow\rangle$ and $|4\rangle = |\downarrow,\downarrow\rangle$. See blue (dashed) line. At larger V_{DC} ($V_{DC} \geq 6$ meV) the chemical potential of the drain crosses the inter-dot triplet state and the right QD becomes suddenly discharged. This produces a large peak in the current and a dramatic reduction in the occupation of states $|3\rangle$ and $|4\rangle$ as expected. At the same time other states, which are now important in the transport, increase their occupations.

The expressions we propose for the the electronic spin-flip scattering rate $W^{sf}_{i,j}$ depend on the different processes:

$$|\downarrow,\downarrow\rangle \rightarrow |\uparrow,\downarrow\rangle \;\Rightarrow\; W^{sf}_{5,4} = \left[\frac{1}{\tau_{sf}}\right]_L \left[\frac{1+P_L}{2}\right] \quad (16)$$

$$|\downarrow,\downarrow\rangle \rightarrow |\downarrow,\uparrow\rangle \;\Rightarrow\; W^{sf}_{6,4} = \left[\frac{1}{\tau_{sf}}\right]_R \left[\frac{1+P_R}{2}\right] \quad (17)$$

$$|\uparrow,\uparrow\rangle \rightarrow |\uparrow,\downarrow\rangle \;\Rightarrow\; W^{sf}_{5,3} = \left[\frac{1}{\tau_{sf}}\right]_R \left[\frac{1-P_R}{2}\right] \quad (18)$$

$$|\uparrow,\uparrow\rangle \rightarrow |\downarrow,\uparrow\rangle \;\Rightarrow\; W^{sf}_{6,3} = \left[\frac{1}{\tau_{sf}}\right]_L \left[\frac{1-P_L}{2}\right] \quad (19)$$

The equations that describe the time evolution of the nuclei spin polarization for both dots include the flip-flop interaction and a phenomenological nuclear spin relaxation time $\tau_{relax} \approx 100s$ [21] for the scattering between nuclei:

$$\dot{P}_L = W^{sf}_{6,3}\rho_3 - W^{sf}_{5,4}\rho_4 - \frac{P_L}{\tau_{relax}} \quad (20)$$

$$\dot{P}_R = W_{5,3}\rho_3 - W^{sf}_{6,4}\rho_4 - \frac{P_R}{\tau_{relax}} \quad (21)$$

Including spin-flip interactions, the rate equation for the occupation probability of $|3\rangle = |\uparrow,\uparrow\rangle$ and $|4\rangle = |\downarrow,\downarrow\rangle$ is:

$$\dot{\rho}_3 = W_{3,1}\rho_1 + W_{3,7}\rho_7 + W_{3,11}\rho_{11} - \left(W_{1,3} + W_{7,3} + W_{11,3} + W^{sf}_{5,3} + W^{sf}_{6,3}\right)\rho_3 \quad (22)$$

$$\dot{\rho}_4 = W_{4,2}\rho_2 + W_{4,8}\rho_8 + W_{04,12}\rho_{12} - \left(W_{2,4} + W_{8,4} + W_{12,04} + W^{sf}_{5,4} + W^{sf}_{6,4}\right)\rho_3 \quad (23)$$

Total current expression

The system of time evolution equations for the electronic states occupations ρ_i and nuclei polarization of the left and right dot is self-consistently solved. From that we calculate the total current through the system which is the physical observable of interest. The current

going from the left lead to the left QD is defined as:

$$I_L = I_L^{\uparrow} + I_L^{\downarrow} =$$
$$e\{(W_{3,1}\rho_1 + W_{5,2}\rho_2 + W_{14,12}\rho_{12} + W_{16,13}\rho_{13})$$
$$-(W_{1,3}\rho_3 + W_{2,5}\rho_5 + W_{12,14}\rho_{14} + W_{13,16}\rho_{16})\}^{\uparrow}$$
$$+e\{(W_{6,1}\rho_1 + W_{4,2}\rho_2 + W_{17,12}\rho_{12} + W_{15,13}\rho_{13})$$
$$-(W_{1,6}\rho_6 + W_{2,4}\rho_4 + W_{12,17}\rho_{17} + W_{13,15}\rho_{15})\}^{\downarrow} \quad (24)$$

where the first (second) bracket, $\{\}^{\uparrow}(\{\}^{\downarrow})$, represents the up (down) current. Similar expressions can be obtained for the inter-dot current (I_{12}) and for the current going from the right dot to the collector (I_R). In general the total current through the device is:

$$I = \frac{I_L + I_{1,2} + I_R}{3} \quad (25)$$

III. RESULTS

Experimental results[1] show, for magnetic field B=0, a peak at low V_{DC}, a big plateau and a peak of high intensity at large V_{DC}, ($V_{DC} \geq 6$ meV). We present similar calculated results in Fig. 2. At low V_{DC}, I takes place when one electron from the (1,1) spin-singlet, tunnels to the double occupied singlet state in the right QD (0,2). This process happens when the extra energy to add one electron to the right QD is given by a nearby gate voltage. At higher V_{DC} the system reaches the states $|3\rangle = |\uparrow,\uparrow\rangle$ and $|4\rangle = |\downarrow,\downarrow\rangle$ (inter-dot triplet states) and I drops off due to SB. It corresponds to the observed plateau. This can be observed in Fig. 3, where the state occupation is presented versus applied bias. According to it, the SB region is governed by the states $|3\rangle$ and $|4\rangle$ with an occupation of almost 0.5 for each state. In this V_{DC} region the only way for one electron in the left QD to tunnel to the right one would be through an excited state in the right QD. Nevertheless at zero B, is too high in energy to participate in the transport window. Despite SB, there is a finite leakage current measured in the SB region due to the finite probability for electrons in the QD's to flip their spin by interaction with nuclei. At larger V_{DC} ($V_{DC} \geq 6$ meV) the chemical potential of the right lead crosses the inter-dot triplet state and the right QD becomes suddenly discharged producing a large peak in the current. This peak is mainly due, according to our calculations, to the inelastic contribution to the current with the emission of acoustic phonons. The elastic contribution is rather small because the ground levels in each dot involved in the tunneling :$|\uparrow,0\rangle \rightarrow |0,\uparrow\rangle$ and $|\downarrow,0\rangle \rightarrow |0,\downarrow\rangle$, are totally out of resonance. This situation corresponds very well with the schematic diagram in the Fig. 1a.

A finite B parallel to the current, produces an energy shift experienced by the Fock-Darwin states due to its coupling with the electronic orbital momentum. B couples with the electronic orbital angular momentum of the first excited state of the right QD ($l = 1$). An additional shift in the electronic energy comes as well from the additional confinement potential induced by B [22]. These B-dependent shifts and the typical energy scales of this problem (on-site Coulomb energy or orbital level spacing) are much larger than the Zeeman splitting. Thus, Zeeman splitting is neglected only in terms of tunneling processes. Increasing B the first excited state of the right QD (0, $\uparrow\uparrow^*$) enters in the transport window and comes

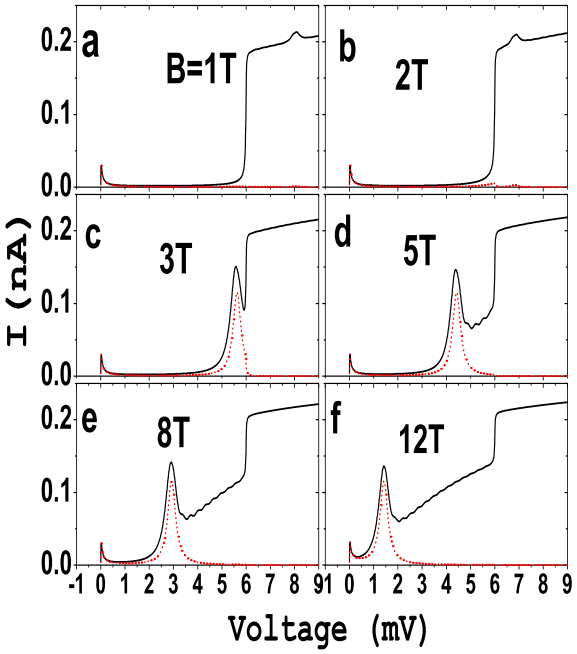

FIG. 4: (Color on line). Stationary I/V_{DC} curve calculated for different B. We observe an additional peak at finite B which moves to lower V_{DC} as B increases. For different values of B the resonance condition: $|3\rangle = |\uparrow,\uparrow\rangle \Rightarrow |7\rangle = |0,\uparrow\uparrow^*\rangle$ and $|4\rangle = |\downarrow,\downarrow\rangle \rightarrow |8\rangle = |0,\downarrow\downarrow^*\rangle$ occurs at different values of V_{DC}. A shoulder at the right side of the B-dependent peak is also observed. The single line corresponds to both elastic transitions (direct tunneling) and inelastic transitions (phonon-assisted contributions). The dotted line means that only elastic transitions are taken into account. In this case it can be observed that the shoulder and the large right peak collapses. This demonstrates that inelastic transitions play a crucial role to sustain the current not only in the large right peak, but also in the right shoulder of the moving central peak. Again elastic inter-dot transitions do not contribute because the corresponding levels in each dot are out of resonance. The resonant peaks move to lower V_{DC} as B increases as expected. For larger B the energy shift for the excited state is also larger and its final position is getting closer to the ground state. As a result a lesser V_{DC} is required to get the resonant condition.

into resonance with the ground state of the left QD. This opens a new transport channel, and thus I flows through the device and SB is lifted. In Fig. 4 we present the stationary I/V_{DC} curve calculated for different B. We observe an additional peak at finite B which moves to lower V_{DC} as B increases. For different values of B, the resonance condition occurs at different values of V_{DC}. In Fig. 4, the single line corresponds to both elastic (direct tunneling) and inelastic (phonon-assisted) contributions. The dotted line represents only elastic inter-dot transitions. According to these results, inelastic transitions play a crucial role to sustain the current. They are responsible of the large right peak and the right shoulder of the moving central peak. In the latter, elastic inter-dot transitions do not contribute because the corresponding levels in each dot are out of resonance (See fig. 1b). The results presented in Fig. 4 are in good agreement with the experimental curve by Ono et al.[1], including the shoulder at the right side of the B-dependent peak. The oscillations however are smeared out in the experiment. The reason being that we did not include in our model damping of the bosonic system corresponding to phonon cavity losses[23]. It has been shown that the system is extremely sensitive even to very small damping[23].

Fig. 5 shows the charge occupation for different states and for the same values of B as in Fig. 4. For small B the electrons occupy mainly the inter-dot triplet states ($|\uparrow,\uparrow\rangle$ and $|\downarrow,\downarrow\rangle$) in the SB region with a probability of almost 0.5 for each one. No SB removal is observed apart from a finite leakage current due to sf by HF interaction. In this case the resonant condition between the ground state of the left dot and the first excited state of the right dot ($|\uparrow,\uparrow\rangle \Rightarrow |0,\uparrow\uparrow^*\rangle$ or $|\downarrow,\downarrow\rangle \Rightarrow |0,\downarrow\downarrow^*\rangle$), is fulfilled at $V_{DC} > 6mV$. However at larger B the resonant condition happens inside the SB region giving rise to blockade lifting. The opening of this new current channel corresponds to a decrease in the occupation of $|3\rangle$ and $|4\rangle$ and to an increase in the occupation of $|7\rangle$ and $|8\rangle$. The shoulder at the right side of the resonant peak produces also a removal of SB. This is due to inelastic tunneling through the inner barrier assisted with the emission of acoustic phonons. Summarizing, SB removal is produced by three processes: the first one is electronic spin-flip by HF interaction. The second one is elastic tunneling through the right dot excited state coming into the transport window by B. Finally, additional inelastic contributions to the inner tunneling assisted by emission of acoustic phonons.

The microscopical model for the Hyperfine interaction, allows us to study the dynamical nuclear polarization in each dot[24]. We calculate the nuclear polarizations $P_{L(R)}$, versus the applied voltage and different magnetic fields. We have considered that $N_L = 10^6$ and $N_R = 1.1 \times 10^6$. As a consequence we obtain different spin-flip rates for each dot. We present the obtained results in Figs. 6 and 7. In Fig. 6 we represent the

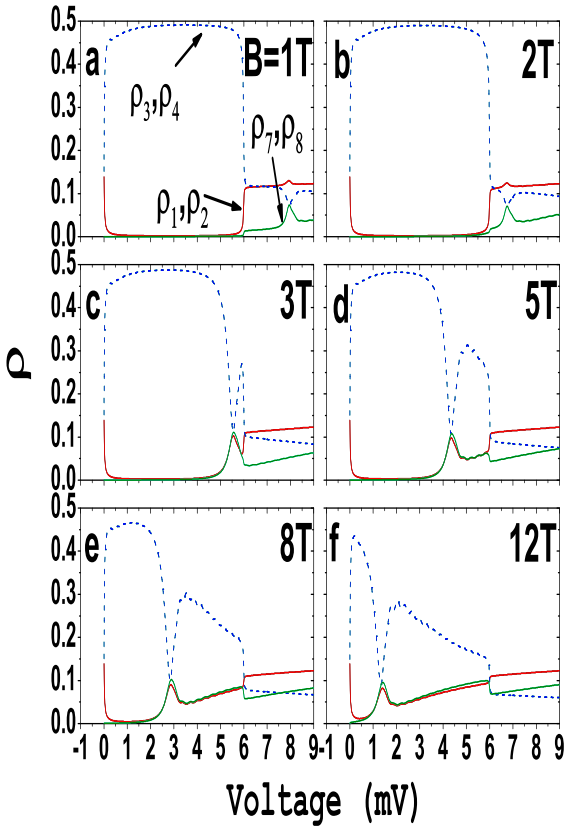

FIG. 5: (Color on line). Stationary charge occupation of the electronic states for the same cases of B as in Fig. 4. In the SB region the inter-dot triplet states($|3\rangle$ and $|4\rangle$) are occupied in the QD's, for lower values of B. For larger B the resonant condition between the ground state of the left QD and the excited state of the right QD is fulfilled inside the SB region. This give rise to spin blockade removal. The opening of this new current channel decreases ρ_3 and ρ_4 and increases ρ_7 and ρ_8

nuclear polarizations of left and right dot versus applied voltage for four different B separately $B = 2, 3, 5$ and $8T$. As we said above, for $B \neq 0$ only electronic spin-flip relaxation process are possible: from spin down to spin up. This means that for nuclei we have the opposite process, i.e., from spin up to spin down that explains the negative nuclear polarization. For all magnetic fields studied, the right dot presents an smaller negative polarization. This is because of the larger number of nuclei in the right dot (see eqn. (12)). The peculiar shape that these graphs present can be explained if we rewrite the dynamical equations of the nuclear polarization of left and right dot. Now we have to take into account that only electronic spin-flip relaxation processes are allowed and that the nuclear spin relaxation time is very large.

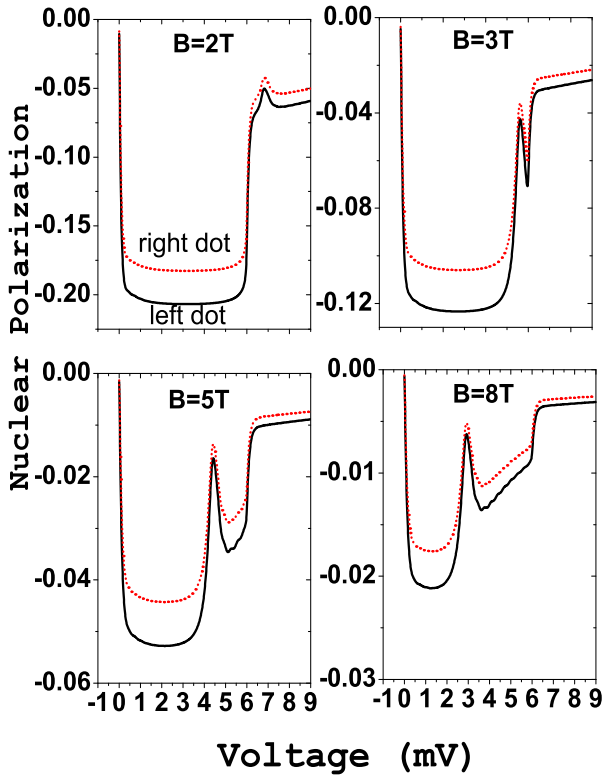

FIG. 6: (Color on line). Nuclear polarizations of left and right dot versus applied voltage for four different B separately $B = 2, 3, 5$ and $8T$. For $B \neq 0$ only electronic spin-flip relaxation process are possible: from spin down to spin up. For the nuclei we have the opposite process: from spin up to down. This explains the negative polarization obtained for both dots. The variation of $P_L(R)$ is opposite to the electronic occupation of state $|4\rangle$ as expected. The decreasing polarization magnitude versus increasing B is a consequence of the splitting Zeeman (see eqn. 13)).

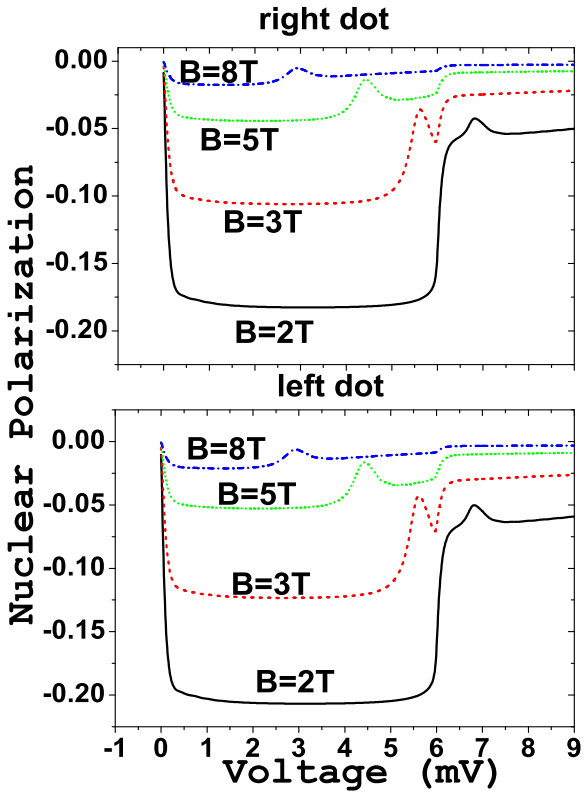

FIG. 7: (Color on line). Nuclear polarization for both dots and all magnetic fields jointly. The negative values of $P_L(R)$ decrease as the magnetic field increases. This happens in both dots. If we increase B, ΔZ_e increases and consequently spin-flip rate and nuclear polarization decrease as expected.

Finally the two equations read:

$$\dot{P}_L = -W^{sf}_{5,4}\rho_4 \quad (26)$$

$$\dot{P}_R = -W^{sf}_{6,4}\rho_4 \quad (27)$$

According to these expressions the calculated values for $P_L(R)$ versus applied voltage are opposite to ones obtained for ρ_4. That means that when the occupations of state $|4\rangle$ increases (SB region) nuclear polarization should increase (in negative) too. However, outside of the SB region or when the SB is removed (new transport channel through state $\rho_8 = |0, \downarrow\downarrow^*\rangle$) nuclear polarization decreases because ρ_4 is much smaller.

In Fig. 7, we present in two panels the nuclear polarization for both dots and all magnetic fields jointly. The negative values of $P_L(R)$ decrease as the magnetic field increases. This happens in both dots. The explanation comes readily if we observe the expression of the spin-flip scattering rate (eqn. 13). The highest values for this rate corresponds to an splitting Zeeman $\Delta Z_e \simeq 0$, that is obtained at $B = 0$. In this situation spin down and spin up electronic states are degenerate. However if we increase B, ΔZ_e increases and consequently spin-flip rate and nuclear polarization decrease. Summarizing, we obtain a dynamical nuclear polarization that is intimately related with the electronic occupation through the device.

IV. CONCLUSIONS

In conclusion we reproduce experimental features by Ono et al.[1], and show how, inelastic transitions with the corresponding emission of phonons play a crucial role sustaining the current through the device. We show as well that the interplay between the electron and nuclei spin distributions within the dots are responsible for lifting the SB yielding a leakage current. We demonstrate also that at finite B, the participation of excited states in

the current lifts SB. We develop a microscopical model to account for the Hyperfine interaction in each dot. Using this model we study the dynamical nuclear polarization as a function of the applied voltage. We obtain that nuclear polarization is closely related with the electronic occupations. Our results indicate that a combination of B and V_{DC} allows to control the current through the device, making these systems potential components for spintronics and quantum computing.

ACKNOWLEDGMENTS

This work has been supported by the MCYT (Spain) under grant MAT2005-06444 (JI and GP), by the Ramón y Cajal program (J.I.) by the EU Human Potential Programme: HPRN-CT-2000-00144, by the Welch Foundation (AHM) and by the DOE (AHM) under grant DE-FG03-02ER45958.

[1] K. Ono, D.G. Austing, Y. Tokura and S. Tarucha, Science **297** 1313 (2002).

[2] A.C. Johnson, J.R. Petta, C.M. Marcus, M.P. Hanson and A.C. Gossard, Phys. Rev. B, **72** 165308 (2005).

[3] Toshimasa Fujisawa, David Guy Austing, Yasuhiro Tokura, Yoshiro Hirayama, Seigo Tarucha , Nature (London) **419**, 278 (2002); R. Hanson, B. Witkamp, L. M. K. Vandersypen, L. H. Willems van Beveren, J. M. Elzerman, and L. P. Kouwenhoven., Phys. Rev. Lett.,**91**, 196802 (2003); J. M. Elzerman, R. Hanson, L. H. Willems van Beveren, B. Witkamp, L. M. K. Vandersypen, L. P. Kouwenhoven , Nature, **430**, 431 (2004).

[4] Oliver Gywat, Hans-Andreas Engel, Daniel Loss, R. J. Epstein, F. M. Mendoza, and D. D. Awschalom, Phys. Rev. B, **69**, 205303 (2004).

[5] Vitaly N. Golovach, Alexander Khaetskii, and Daniel Loss , Phys. Rev. Lett., **93**, 016601 (2004).

[6] Sigurdur I. Erlingsson, Yuli V. Nazarov, and Vladimir I. Falko , Phys. Rev. B, **64**, 195306 (2001); *ibid*, Phys. Rev. B, **66**, 155327 (2002); *ibid*, Phys. Rev. B, **72**, 033301 (2005);Alexander V. Khaetskii and Yuli V. Nazarov , Phys. Rev. B, **61**, 12639 (2000).

[7] E Cota, R Aguado, C E Creffield and G Platero, Nanotechnology **14**, 152 (2003); Ernesto Cota, Ramn Aguado and Gloria Platero , Phys. Rev. Lett., **94**, 107202 (2005).

[8] K. Blum. *Density Matrix Theory and Applications.* (New York:Plenum) 1981

[9] Gnter Mahler and Volker A. Weberru, *Quantum Networks: Dynamics of Open Nanostructures.* (Berlin:Springer) 1995

[10] Hans-Andreas Engel and Daniel Loss , Phys. Rev. B **65**, 195321 (2002)

[11] Bing Dong, X. L. Lei, Phys. Rev. B 66, 113310 (2002)

[12] W. G. van der Wiel, S. De Franceschi, J. M. Elzerman, T. Fujisawa, S. Tarucha and L. P. Kouwenhoven , Rev. Mod. Physics **75** 1 (2003).

[13] S. A. Gurvitz and Ya. S. Prager, Phys.Rev. B **53** 15932 (1996).

[14] Toshimasa Fujisawa, Tjerk H. Oosterkamp, Wilfred G. van der Wiel, Benno W. Broer, Ramn Aguado, Seigo Tarucha, and Leo P. Kouwenhoven, Science, **282**, 932, (1998).

[15] Y.V. Nazarov, Phys. B, **189**, 57-69 (1993).

[16] T. H. Stoof and Yu. V. Nazarov, Phys. Rev. B, **53**, 1050 (1996).

[17] N. C. van der Vaart, S. F. Godijn, Y. V. Nazarov, C. J. P. M. Harmans, J. E. Mooij, L. W. Molenkamp, C. T. Foxon, Phys. Rev. Lett., **74**, 4702 (1995).

[18] T. Brandes and B. Kramer, Phys. Rev. Lett., **83**, 3021, (1999); T. Brandes, Phys. Rep., **408**, 315-408, (2005).

[19] D. Paget, G. Lampel and B. Sapoval, Phys. Rev. B **15**, 5780 (1977).

[20] Sigurdur I. Erlingsson, and Yuli V. Nazarov, Phys. Rev. B **64**, 195306 (2001).

[21] K. Ono, S. Tarucha, Phys. Rev. Lett. 92, 256803, (2004); F.H.L. Koppens et al., Science, **309**, 1346 (2005).

[22] L. P. Kouwenhoven, T. H. Oosterkamp, M. W. S. Danoesastro, M. Eto, D. G. Austing, T. Honda, and S. Tarucha , Science, **278**, 1788 (1997).

[23] T. Brandes and N. Lambert, Phys. Rev. B, **67**, 125323 (2003).

[24] M.S. Rudner and L.S. Levitov, cond-mat/0609409; M.S. Rudner and L.S. Levitov, cond-mat/07052177.